



Interface, lattice strain and dislocation density of SiC_p/Al composite consolidated by equal channel angular pressing and torsion

Chen-hao QIAN, Ping LI, Ke-min XUE

School of Materials Science and Engineering, Hefei University of Technology, Hefei 230009, China

Received 15 August 2014; accepted 27 October 2014

Abstract: Powder mixture of pure Al and oxidized SiC was consolidated into 10% (mass fraction) SiC_p/Al composites at 523 K by equal channel angular pressing and torsion (ECAP-T). The interfacial bonding of the composites was characterized by transmission electron microscopy (TEM) and high resolution transmission electron microscopy (HRTEM). The selected area electron diffraction (SAED) for the interface was investigated. The elements at the interface were scanned by energy dispersive spectroscopy (EDS) and the EDS mapping was also obtained. X-ray diffraction (XRD) analysis was carried out for the composites fabricated by 1 pass, 2 passes and 4 passes ECAP-T. According to the XRD analysis, the influences of ECAP-T pass on the Bragg angle and interplanar spacing for Al crystalline planes were studied. The results show that after ECAP-T, the interface between Al and SiC within the composites is a belt of amorphous SiO₂ containing a trace of Al, Si and C which diffused from the matrix and the reinforcement. With the growing ECAP-T pass, the Bragg angle decreases and interplanar spacing increases for Al crystalline planes, due to the accumulated lattice strain. The increasing lattice strain of Al grains also boosts the density of the dislocation within Al grains.

Key words: metal matrix composites; severe plastic deformation; interface; lattice strain; dislocation density

1 Introduction

In recent years, particle reinforced metal matrix composites (PRMMCs) have gained much attention because of their attractive properties. Among these composites, Al matrix composites have received intense attention in the past few decades due to their high specific stiffness, strength and superior wear resistance [1–3]. Since the raw materials of these composites are always powders, powder metallurgy (P/M) is often taken into account as a method for fabricating these composites [4,5]. However, the composites fabricated by P/M are always have a certain amount of pores, which need to experience some consequent processing to diminish these pores [6–9]. In order to simplify and optimize the fabrication process, a new method named as severe plastic deformation (SPD) was proposed. As one of the most commonly employed methods in SPD, equal channel angular pressing (ECAP) was applied to achieving composites reinforced by carbon nanotube. The ECAP treated composites presented qualified relative density and wonderful

mechanical properties [10]. Based on these experiment results, some novel ECAP processes for composites consolidation were developed. SiC_p/Al composites were consolidated from Al and SiC powders by a special ECAP method, forward extrusion and equal channel angular pressing (FE-ECAP). The as-consolidated composites have better compaction performance than the same composites consolidated by hot forward extrusion [11]. Another special ECAP method, back pressure equal channel angular pressing (BP-ECAP) was engaged to fabricate Al matrix composite by reinforced Al₂O₃ particulates. The as-consolidated composites also have perfect compaction performance, which was mainly attributed to the interaction interface caused by severe shear deformation [12].

In this work, SiC_p/Al composites were consolidated from mixed powders of SiC and Al by a kind of improved ECAP process named as equal channel angular pressing and torsion (ECAP-T). As shown in Fig. 1, the ECAP-T die consists of two intersected square channels and a spiral channel. This process was originally designed for consolidating pure Al powder and proved as a feasible approach for fabricating fully dense bulk

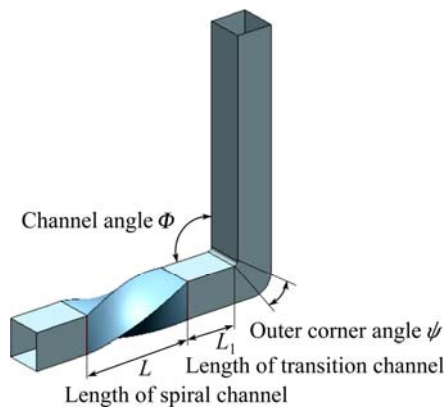


Fig. 1 Schematic illustration of ECAP-T process

material with fine grains [13]. Then this process was tested for consolidating the mixture of SiC particles and Al powders and the tests show that ECAP-T process can achieve qualified composites with high relative density [14]. But the consolidated interfaces of this kind of composites have not been studied. The aim of this study is to investigate the interfacial composition of SiC_p/Al composites consolidated by this process. The influences of ECAP-T pass on the lattice parameter, the lattice strain and the dislocation density of the Al grains in the composites were studied.

2 Experimental

High purity (99.81%) Al powder having an average particulate size of 32.22 μm was chosen for raw matrix material. The main impurities in Al were 0.11% Fe and 0.07% Si. The reinforcement used in this study was 3C-SiC having an average particulate size of 13.59 μm, and the main impurity was 6H-SiC. The temperature at which SiC_p/Al composites were fabricated via ordinary PM method was always around the melting point of Al, therefore, it was difficult to inhibit the harmful reaction at the interface between Al and SiC. The interfacial phase Al₄C₃ forming in the reaction is a kind of brittle compound which can weaken the bonding strength of SiC/Al interface. In this study, though the ECAP-T processing temperature is much lower, the severe hydrostatic pressure may support the driving power of the harmful reaction which is equal to the thermal power during PM processing. Therefore, the pretreatment of SiC powders is necessary. SiC powders were pre-heated in a furnace at 523 K for 2 h to remove the moisture and then oxidized at 1023 K for 2 h to form oxidation layer on the particle surface. This layer can avoid the reaction discussed above.

Then, the oxidized SiC powder was homogeneously blended with the matrix Al powder in the mass ratio of 9:1. The morphology of the mixture of Al powders and SiC particles is shown in Fig. 2. As can be seen, the

blended powders had a random morphology. Al and SiC particles were near-ball and polygon-like, respectively. The powder mixture was wrapped in copper tubes with a relative density of 0.7 and then inserted into ECAP-T die with a 10 mm × 10 mm cross-section. The ECAP-T process was carried out at 523 K under inert gas protection with a ram speed of 1 mm/s in single pass, 2 passes and 4 passes, following route B_C (the sample is rotated by 90° in the same direction between consecutive passes). The reason for choosing B_C route is that an optimum homogeneous microstructure of equiaxed grains, separated by high angle grain boundaries, is attained most readily among the four kinds of routes (A, C, B_A and B_C). During the pressing, the mixed lubricant of graphite and MoS₂ was engaged in order to reduce the friction. The die parameters are listed in Table 1. The load applied on the samples is about 78.4 kN, provided by the hydraulic press (RZU2000HF, Hefei Metalforming Machine Tool Co., Ltd).

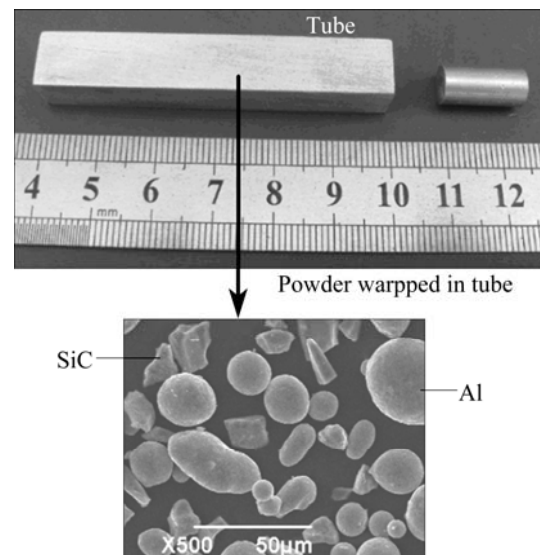


Fig. 2 SEM image of powder mixture

Table 1 Die parameters

Channel angle, $\Phi/(\circ)$	Outer corner angle $\psi/(\circ)$	Twist angle/ (\circ)	Length of spiral channel L/mm	Length of transition channel L_1/mm
90	37	90	30	15

In this study, transmission electron microscopy (TEM) and high resolution transmission electron microscopy (HRTEM) were employed for examining the interfacial bonding of the as-consolidated composites as well as the distribution of the dislocation within Al grains. The sizes of the samples for TEM and HRTEM are $d3\text{mm} \times 50 \mu\text{m}$. The macrophotographs of the samples are shown in Fig. 3, and it can be seen that all the samples are consolidated well. Selected area electron diffraction (SAED) was combined with energy dispersive

spectroscopy (EDS) in order to determine the interfacial composition. X-ray diffraction (XRD) was used for analyzing the interplanar spacing and Bragg angle of Al grains within the initial powder mixture and the composites fabricated by different passes. According to the XRD analysis, the quantitative calculations for the lattice strain and dislocation density of Al grains in the composites were carried out.

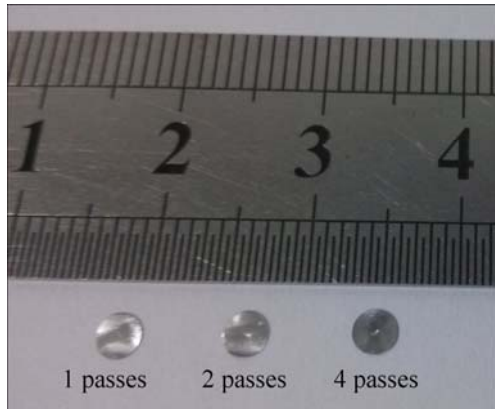


Fig. 3 Macro photographs of composites

3 Results and discussion

Figures 4(a)–(c) show the composites containing 10% SiC consolidated by 1 pass, 2 passes and 4 passes ECAP-T, respectively. It can be seen that SiC particulates disperse in Al matrix more homogeneously as the number of ECAP-T pass grows. The average size of SiC particulates and the amount of SiC clusters both decrease with the increase of ECAP-T pass. As shown in Figs. 5(a) and (b), the shield stress and the microhardness of the composites both increase with ECAP-T pass in the ranges of 104–117 MPa and HV 46.5–53.8, respectively.

3.1 Interface of composites

TEM bright-field image is shown in Fig. 6(a) for the SiC/Al composites fabricated by single pass ECAP-T. It is seen that the SiC particulates can be clearly distinguished from the Al matrix due to their different image contrasts. And the SiC particulates in the image are wrapped by a bright belt. From the further magnified image (Fig. 6(b)), the thickness of the belt was measured as about 80 nm. In order to figure out what kind of substance the belt belongs to, the corresponding SAED patterns of the TEM image were examined. Due to the limit of the equipment, the diameter of the SAED area has a minimum value of 100 nm. Therefore, the selected area cannot be restricted in the bright belt and it must contain a small amount of SiC or Al. Three circle zones shown in Fig. 6(b) were selected at the positions of SiC (Zone I), Al (Zone II) and the belt (Zone III) for SAED, respectively.

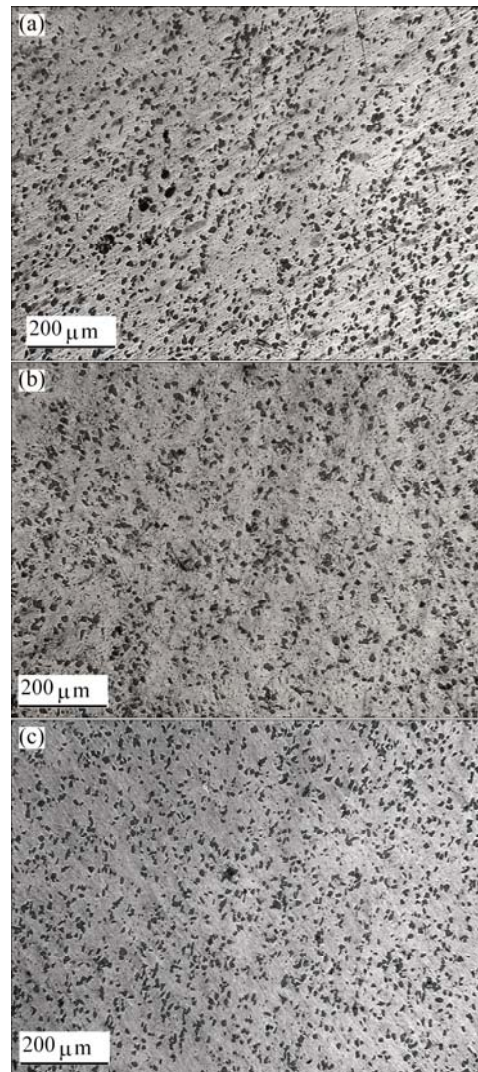


Fig. 4 Microphotographs of composites (10% SiC) processed by 1 pass (a), 2 passes (b) and 4 passes (c) ECAP-T treated at 250 °C

Figure 7 shows the SAED patterns for there selected zones discussed above. The distance from the center of SAED pattern to the diffraction spot corresponds to the reciprocal spacing. The distance was measured and transformed into the real spacing (hereafter called d -spacing). It is known that the crystal structure of Al and 3C-SiC belongs to the type of face-centered cubic (FCC). Thus, according to the value of d -spacing, we can determine the crystal plane which corresponds to the diffraction spot. As shown in Figs. 7(a) and (b), we can determine $\{111\}$ and $\{200\}$ planes of 3C-SiC and Al. It should be noted that these crystal planes can also be observed in the SEAD patterns of Zone III (Fig. 7(c)) and the reason is discussed above that the diffraction area embraces SiC and Al. Meanwhile, several diffused rings appear in Fig. 7(c) and cannot be observed in Figs. 7(a) and (b). They are concentric with each other and the boundary of each ring is blurry. These diffused rings are

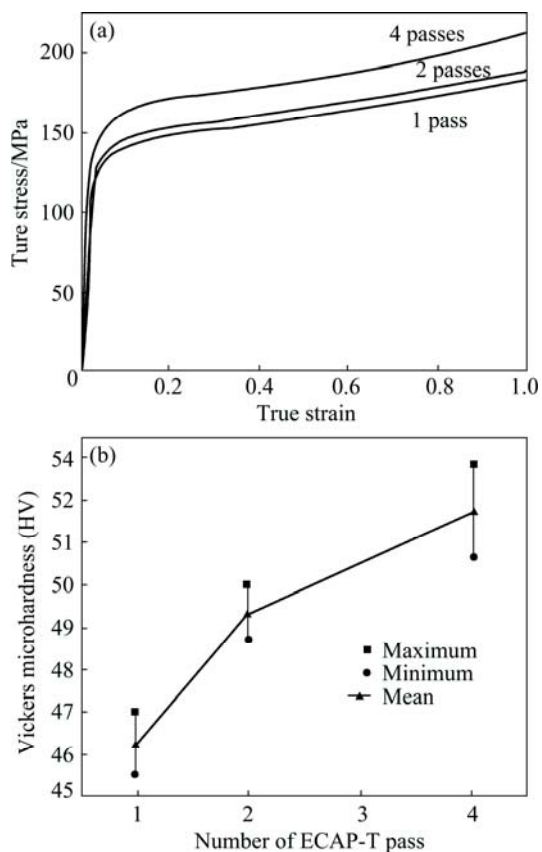


Fig. 5 Compression curves (a) and hardness values (b) of composites (10% SiC) processed by 1, 2 and 4 passes ECAP-T

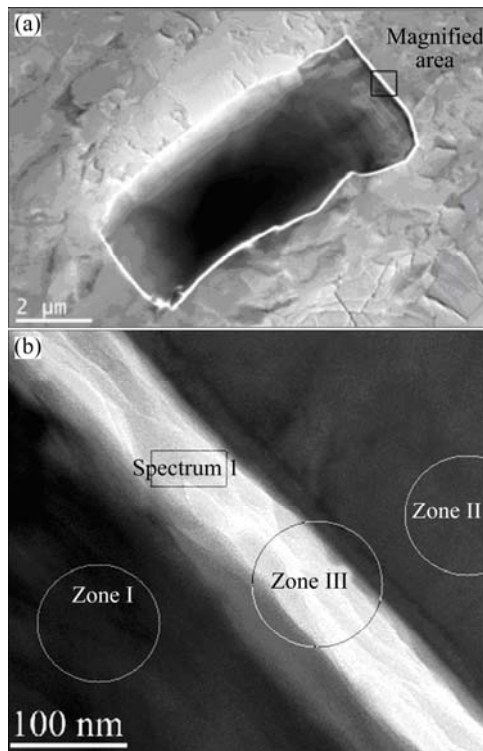


Fig. 6 TEM bright-field images of composites fabricated by 1 pass ECAP-T (a) and local magnification for interface of SiC and Al (b)

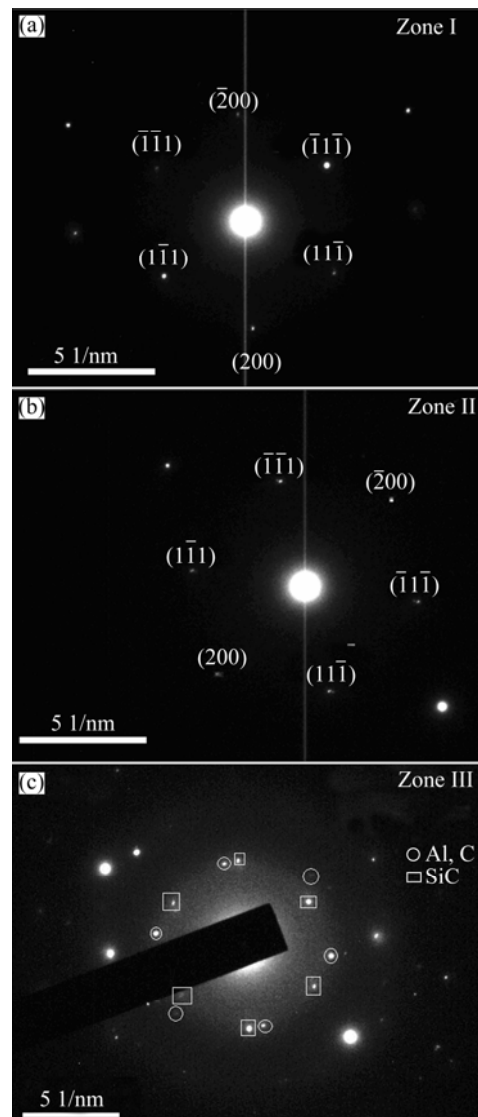


Fig. 7 SAED patterns for Zone I (a), Zone II (b) and Zone III (c)

in accordance with the typical characteristic of amorphous phase. It can be inferred that the bright belt in Fig. 6 is a kind of amorphous substance. The TEM samples were fabricated by mechanical polishing and ion-thinning, therefore, no substances contaminate the samples and this amorphous substance cannot be introduced from outside. The HRTEM image of this phase is shown in Fig. 8. It is observed that the phase has a kind of disordered punctate structure which is different from the laminated structure of SiC. It further proves that the structure of the belt phase at the interface belongs to amorphous state instead of the crystalline state of the matrix or reinforcement.

TEM-EDS mapping of possible elements by scanning the whole area of Fig. 6(b) was carried out and it is found that the element O, which hardly exists in the matrix and reinforcement, concentrates in the belt phase as shown in Fig. 9(a). EDS spot analysis was then

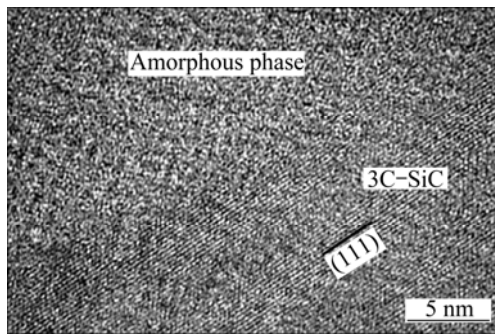


Fig. 8 HREM image of amorphous phase and 3C-SiC at interface of composites

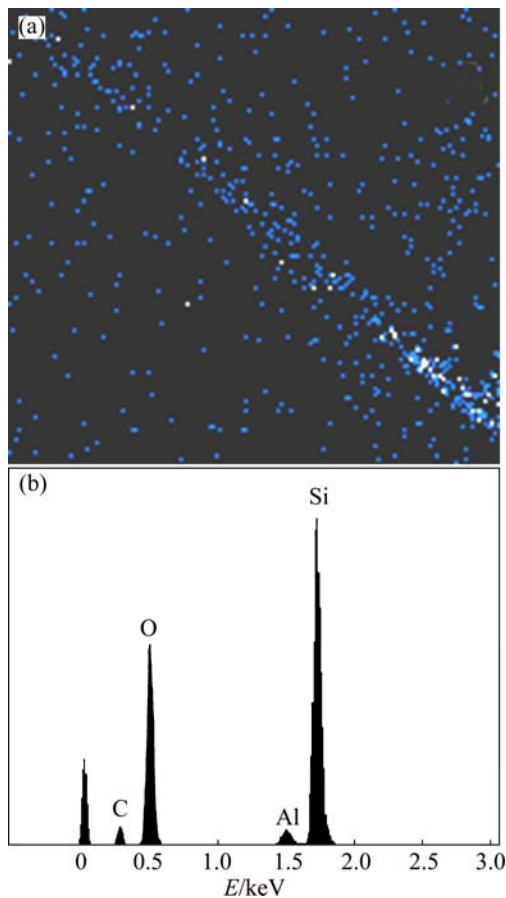


Fig. 9 EDS analysis at interface of composites: (a) EDS mapping of O; (b) EDS spectrum of spot analysis on amorphous phase

carried out at the position located on the belt phase. The corresponding EDS spectrum (Fig. 9(b)) indicates that the phase is rich in Si and O and also contains a trace of Al and C. The chemical compositions of this phase are summarized in Table 2. The mole fractions of Si and O were measured as around 35.29% and 55.5%, respectively. This means that the mole ratio of Si to O is about 1:1.6. According to this ratio, the composition of the amorphous phase can be determined as SiO_2 . Though there is a deviation from the mole ratio (1:2.0) in SiO_2

phase, it should be noted that EDS analysis about light element (like O) is not very accurate. Moreover, the existence of Al and C in the phase proves that the interdiffusion of the elements between the reinforcement and matrix should also be taken into account. Therefore, it can be inferred that a small amount of Si belongs to the SiC particulate also transmitted into the interface, which can increase the mole fraction of Si. Based on the TEM and HRTEM examination discussed above, it can be determined that the interfacial composition between Al and SiC within the composites is an amorphous phase of SiO_2 containing a trace of Al, Si and C diffused from the matrix and the reinforcement.

Table 2 Chemical composition of amorphous phase

Element	w/%	x/%
C	4.05	1.51
O	44.28	55.50
Al	1.85	1.51
Si	49.82	35.29
Sum	100	100

3.2 Lattice strains and dislocation densities of composites

XRD profiles of the initial powder mixture before deformation and after different passes ECAP-T deformation are shown in Fig. 10. Since the element Al occupies about 90% of the composites, the strongest peaks belong to the crystallographic planes of Al which are (1 1 1), (2 0 0), (2 2 0), (3 1 1) and (2 2 2) planes. The planes of 3C-SiC can also be observed, especially the (1 1 1), (2 0 0), and (2 2 0) planes. However, the (3 1 1) and (2 2 2) planes of 3C-SiC are not so obvious. It should be noted that the highest peaks of Al and 3C-SiC both represent (1 1 1) planes, which are main

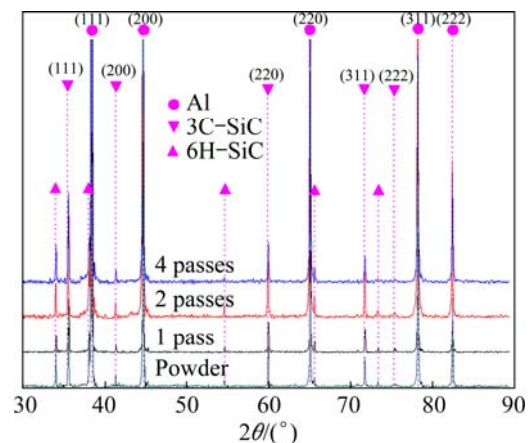


Fig. 10 XRD profiles of SiC_p/Al composites fabricated by 1 pass, 2 passes and 4 passes ECAP-T, including as-received powder mixture

glide planes for FCC crystals. During ECAP-T deformation, preferred orientation along the main glide planes exists in these crystals. There are still some weak peaks, which means that 6H-SiC having a low mass fraction. The grains within SiC particulates were hardly influenced by the ECAP-T deformation, therefore, the crystalline information of the matrix Al will be focused on as below.

A close examination of the XRD profiles indicates that certain peak positions of Al are shifted to somewhat lower angles in the consolidated samples compared with their positions before ECAP-T. This also leads to the change of d -spacing for Al after ECAP-T processing. Variations of Bragg angle and d -spacing as two functions of ECAP-T passes for different crystal planes of Al crystals belonging to the SiC_p/Al composites are plotted in Fig. 11. It is observed that the Bragg angles of the planes decrease with the growing ECAP-T pass. After 4 passes, the Bragg angle changes from 38.449° to 38.363° for (1 1 1) plane, from 44.699° to 44.633° for (2 0 0) plane, from 65.078° to 65.034° for (2 2 0) plane and from 78.210° to 78.167° for (3 1 1) plane. In contrast, the d -spacing of the planes increases with the growing ECAP-T pass. The d -spacing changes from 0.2339 to 0.2345 nm for (1 1 1) plane, from 0.2025 to 0.2028 nm

for (2 0 0) plane, from 0.1412 to 1432 nm for (2 2 0) plane and from 0.1221 to 1222 nm for (3 1 1) plane. These variations can be attributed to two reasons. First, the interdiffusion of the elements between the matrix and the reinforcement after ECAP-T processing, as shown in Fig. 9, leads to lattice expansion of Al. Second, the large fraction of highly strained nanograin boundaries may distort the Al lattices and introduce the lattice expansions, which can improve the dislocation density.

In this study, the lattice expansion was calculated from the full-width at half-maximum (FWHM) values using the Williamson–Hall method [15] after the effect of the $K_{\alpha 2}$ radiation was removed and the inherent peak broadening caused by the radiation of the X-ray diffractometer was subtracted. The FWHM value increases significantly with torsional strain when ECAP-T is used. The peak broadening is important evidence of the occurrence of lattice strain, dislocation generation and grain fragmentation during ECAP-T processing. The lattice strain ε and the dislocation density ρ ($\rho=14.4\varepsilon^2/b^2$, where b is the Burgers vector) are plotted against the number of deformation passes in Fig. 12(a). The lattice strain and the dislocation density increase with the torsional straining and reach levels as high as 0.04% and $2.66 \times 10^{14} \text{ m}^{-2}$ after 4 passes

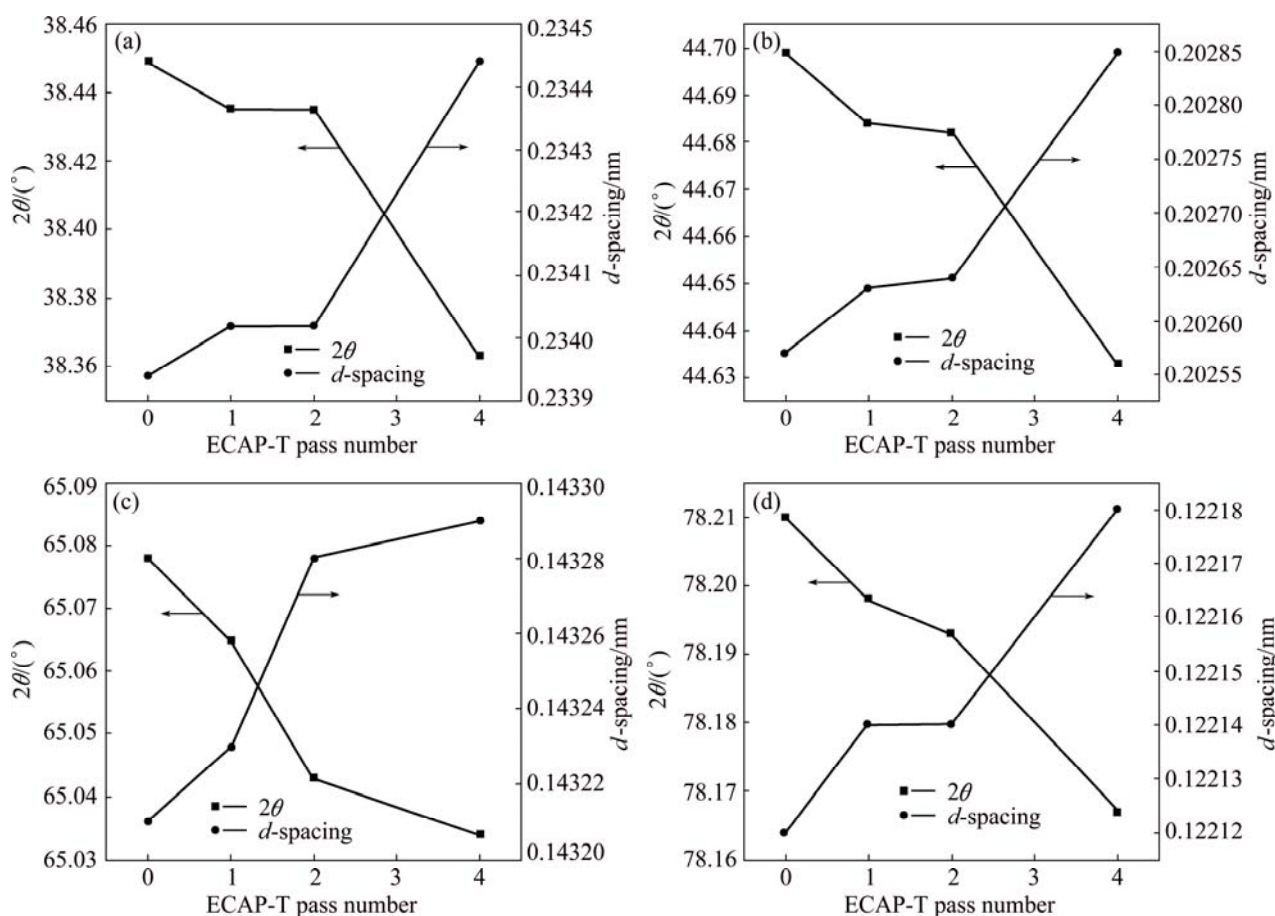


Fig. 11 Variations of Bragg angle and d -spacing as two functions of ECAP-T pass number for (1 1 1) plane (a), (2 0 0) plane (b), (2 2 0) plane (c) and (3 1 1) plane (d) within Al crystals belonging to SiC_p/Al composites

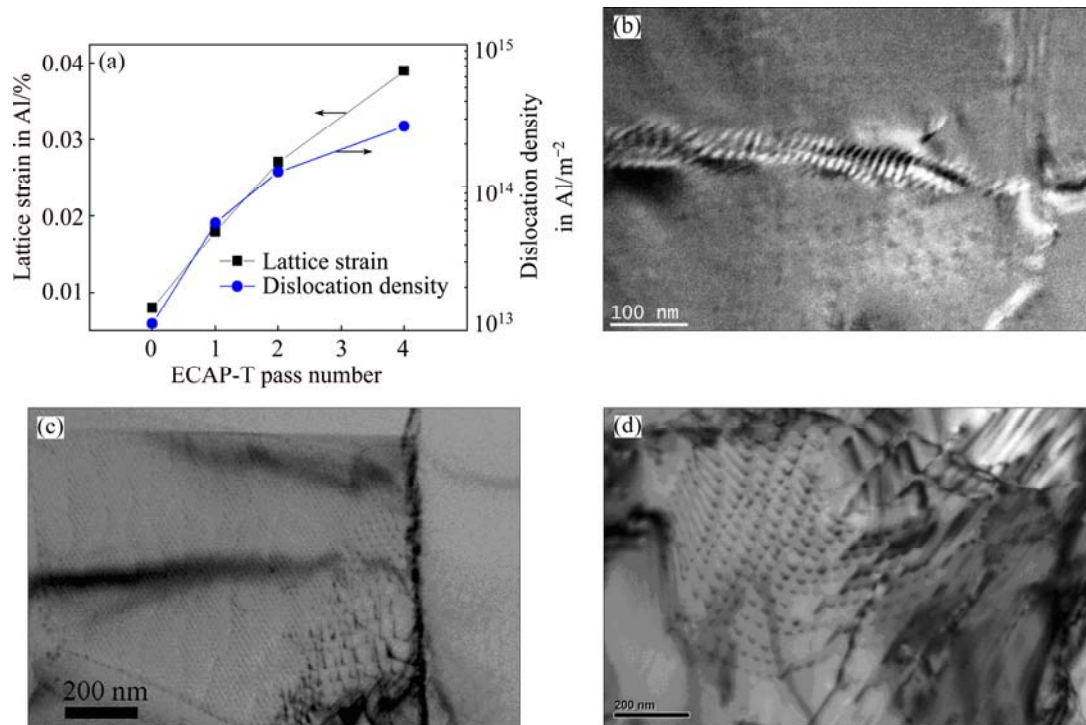


Fig. 12 Variations of lattice strain and dislocation density in Al grains as function of ECAP-T pass number (a), TEM images for composite fabricated by 1 pass (b), 2 passes (c) and 4 passes (d) ECAP-T

deformation. Figures 12(b)–(d) show the TEM images of the interior dislocations in Al grains belonging to the composites consolidated by 1 pass, 2 passes and 4 passes ECAP-T, respectively. It can be directly observed that the amount of dislocations rise up as ECAP-T pass number increases from 1 to 4. Given that these samples have the same gross area, the variation tendency of the dislocation density can be estimated. In Fig. 12(b), the dislocation lines array along the grain boundary and form a dislocation belt with a breadth of about 40 nm. In Fig. 12(c), the dislocation lines along different directions begin to tangle up and spread from the grain boundary into the interior of the grain. In Fig. 12(d), the dislocations appear throughout the Al grain and the dislocation lines form a cellular structure. These observations accord with the variation of dislocation density described in Fig. 12(a).

4 Conclusions

1) Al-based composites (10% SiC) were consolidated from powder mixtures via 1 pass, 2 passes and 4 passes ECAP-T process at 523 K. The shield stress and the microhardness of the composites both increase with ECAP-T pass number in the ranges of 104–117 MPa and HV 46.5–53.8.

2) The interface phase between Al and SiC within the as-consolidated composites is a belt of amorphous SiO₂ containing a trace of other elements (Al, Si and C)

which diffuse from the matrix and the reinforcement.

3) With the growing ECAP-T pass number, the Bragg angle decreases and interplanar spacing increases for Al crystalline planes within the composites.

4) The increasing ECAP-T pass number can enlarge the lattice strain of Al grains and boost the density of the dislocation within Al grains. The corresponding values can reach levels as high as 0.04% and $2.66 \times 10^{14} \text{ m}^{-2}$.

References

- [1] WANG Z, SONG M, SUN C, HE Y. Effect of particle size and distribution on the mechanical properties of SiC reinforced Al–Cu alloy composites [J]. *Materials Science and Engineering: A*, 2011, 528(3): 1131–1137.
- [2] ZHU Meng-jian, LI Shun, ZHAO Xun, XIONG De-gan. Microstructure and properties of SiC_p/Al electronic packaging shell produced by liquid-solid separation [J]. *Transactions of Nonferrous Metal Society of China*, 2014, 24(4): 1039–1045.
- [3] LI Ai-bin, XU Hong-yu, GENG Lin, LI Bing-lin, TAN Zheng-bin, REN Wei. Preparation and characterization of SiC_p/2024Al composite foams by powder metallurgy [J]. *Transactions of Nonferrous Metals Society of China*, 2012, 22(S1): s33–s38.
- [4] PUROHIT R, SAGAR R. Fabrication and testing of Al–SiC_p composite poppet valve guides [J]. *The International Journal of Advanced Manufacturing Technology* 2010, 51(5–8): 685–698.
- [5] KIM S B, KOSS D A, GERARD D A. High cycle fatigue of squeeze cast Al/SiCw composites [J]. *Materials Science and Engineering A*, 2000, 277(1–2): 123–133.
- [6] VALIEV R Z, ISLAMGALIEV R K, KUZMINA N F. Strengthening and grain refinement in an Al-6061 metal matrix composite through intense plastic straining [J]. *Scripta Materialia*, 1999, 40(1):

- 117–122.
- [7] RAMUA G, BAURI R. Effect of equal channel angular pressing (ECAP) on microstructure and properties of Al–SiC_p composites [J]. *Materials & Design*, 2009, 30(9): 3554–3559.
- [8] SABIROV I, PIPPAN R. Formation of a W–25%Cu nanocomposite during high pressure torsion [J]. *Scripta Materialia*, 2005, 52(12): 1293–1298.
- [9] SABIROV I, KOLEDNIK O, VALIEV R Z, PIPPAN R. Equal channel angular pressing of metal matrix composites: Effect on particle distribution and fracture toughness [J]. *Acta Materialia*, 2005, 53(18): 4919–4930.
- [10] QUANG A P, JEONG Y G, YOON S C, HONG S H, KIM H S. Consolidation of 1 vol.% carbon nanotube reinforced metal matrix nanocomposites via equal channel angular pressing [J]. *Journal of Materials Processing Technology*, 2007, 187–188: 46–50.
- [11] MANI B, PAYDAR M H. Application of forward extrusion-equal channel angular pressing (FE-ECAP) in fabrication of aluminum metal matrix composites [J]. *Journal of Alloys and Compounds*, 2010, 492(1–2): 116–121.
- [12] XU W, WUA X, HONMA T, RINGER S P, XIA K. Nanostructured Al–Al₂O₃ composite formed in situ during consolidation of ultrafine Al particles by back pressure equal channel angular pressing [J]. *Acta Materialia*, 2009, 57(14): 4321–4330.
- [13] WANG Xiao-xi, XUE Ke-min, LI Ping, WU Zhan-li, LI Qi. Equal channel angular pressing and torsion of pure al powder in tubes [J]. *Advanced Materials Research*, 2010, 97–101: 1109–1115.
- [14] LI Ping, ZHANG Xiang, XUE Ke-min, LI Xiao. Effect of equal channel angular pressing and torsion on SiC-particle distribution of SiC_p–Al composites [J]. *Transactions of Nonferrous Metals Society of China*, 2012, 22(S2): s402–s407.
- [15] EDALATI K, TOH S, IWAOKA H, HORITA Z. Microstructural characteristics of tungsten-base nanocomposites produced from micropowders by high-pressure torsion [J]. *Acta Materialia*, 2012, 60(9): 3885–3893.

等径角挤扭法制备的 SiC_p/Al 复合材料 界面、晶格畸变和位错密度

钱陈豪, 李萍, 薛克敏

合肥工业大学 材料科学与工程学院, 合肥 230009

摘要: 在 523 K 下, 利用等径角挤扭变形工艺(ECAP-T)将纯 Al 和经氧化处理的 SiC 混合粉末固结成 10% SiC_p/Al 复合材料。采用透射电镜(TEM)和高分辨透射电镜(HRTEM)对所制备的复合材料界面进行观察, 并对相应选区电子衍射花样(SAED)进行标定。利用能谱仪(EDS)对界面结合处进行元素含量测定, 并对试样选区部分进行面分布扫描。采用 X 射线衍射仪(XRD)对不同变形道次(1, 2 和 4 道次)所制备的复合材料进行分析。研究表明, ECAP-T 变形后, Al 和 SiC 之间的界面相属于一种非晶态 SiO₂ 层, 并含有少量从基体和增强颗粒扩散进入的元素 (Al, Si 和 C); 随着 ECAP-T 变形道次的增加, 复合材料中 Al 晶粒的晶格应变不断增加, 导致晶内位错密度增大, 其典型晶面的布拉格衍射角逐渐减小, 而晶面间距逐渐增大。

关键词: 金属基复合材料; 大塑性变形; 界面; 晶格应变; 位错密度

(Edited by Xiang-qun LI)